Computationally efficient model predictive control for quasi-Z source inverter based on Lyapunov function

Minh-Khai Nguyen

Department of Electrical and Electronics Engineering,
Ho Chi Minh City University of Technology and Education,
70000, Vietnam
Email: khainm@hcmute.edu.vn

Kim Anh Nguyen

The University of Danang-University of Science and Technology,
54 Nguyen Luong Bang, Danang, 50000, Vietnam
Email: nkanh@dut.udn.vn

Thi-Thanh-Van Phan

The University of Danang-University of Technology and Education,
48 Cao Thang, Danang, 50000, Vietnam
Email: pttvan@ute.udn.vn

Van-Quang-Binh Ngo*

Faculty of Physics, University of Education,
Hue University,
Thua Thien Hue 49000, Vietnam
Email: nvqbinh@hueuni.edu.vn
*Corresponding author

Abstract: This paper proposes a computationally efficient model predictive control strategy for quasi-Z source inverter. Unlike the classical finite control set model predictive control method, besides the ability of computational cost reduction, the proposed method considers the stability of the closed-loop system in the control design. At each sampling period, only feasible switch control inputs that satisfy the stability condition derived from a control Lyapunov function are taken into account in the minimisation of the cost function. Therefore, the computation time of the optimisation problem is decreased compared with the conventional algorithm. A comparison of the classical model predictive control method is investigated by Matlab software in various operating conditions of the system. The achieved results verify the benefit of the proposed approach for dealing with the stability and computational burden over the conventional method while maintaining high control performance.

Keywords: quasi-Z source inverter; finite control set model predictive control; delay compensation; computational burden; stability condition; control Lyapunov function; efficient optimisation approach; PV system; shoot-through (ST) state; non-ST state.

Reference to this paper should be made as follows: Nguyen, M-K., Nguyen, K.A., Phan, T-T-V. and Ngo, V-Q-B. (2020) 'Computationally efficient model predictive control for quasi-Z source inverter based on Lyapunov function', *Int. J. Modelling, Identification and Control*, Vol. 36, No. 4, pp.342–352.

Biographical notes: Minh-Khai Nguyen received his BS in Electrical Engineering from the Ho Chi Minh City University of Technology, Ho Chi Minh City, Vietnam, in 2005, and the MS and PhD in Electrical Engineering from Chonnam National University, South Korea, in 2007 and 2010, respectively. He was a Lecturer with the Ho Chi Minh City University of Technology and Education, an Assistant Professor with Chosun University, Gwangju, and a research fellow with Queensland University of Technology, Australia. His current research interests include power electronics converters for renewable energy systems and electric vehicles.

Kim Anh Nguyen is currently working as a lecture at The University of Danang-University of Science and Technology (Vietnam) where he held a Head of Automation Division-Faculty of Electrical Engineering from 2009 to 2011. He received his Engineer's degree in Electrical Engineering from

The University of Danang-University of Science and Technology in 2004, MS in Control Engineering and Automation from the University of Danang in 2009, and PhD in systems optimisation and dependability in 2015 from Troyes University of Technology (France). His current research interests are in the cases of stochastic modelling of systems deterioration, prognostic and health management techniques, maintenance and inventory decision-making, optimisation, power electronics, industrial communication networks (IIoT, SCADA), and control systems.

Thi-Thanh-Van Phan received her Bachelor of Engineering in Electronics-Informatics at The University of Danang-University of Science and Technology in 2011, Vietnam. She received her Master's degree in Control Engineering and Automation at The University of Danang-University of Science and Technology, Vietnam, in 2020. From 2011 to 2019, she was a teacher of Vocational College Number 5-Ministry of Defense. In 2020, she is a Lecturer of The University of Danang-University of Technology and Education. Her research interests are in the areas of predictive control and power electronics.

Van-Quang-Binh Ngo received his MSc in 2009 from the Da Nang University of Science and Technology, Vietnam and, the PhD in 2017 from CentraleSupélec-Paris Saclay University, France, all in automation. He was appointed a lecturer at the Hue University of Education, Vietnam in 2004 and promoted to Assistant Professor in 2017. He was a Postdoctoral Researcher at the Department of Electrical Engineering, Chonnam National University, South Korea in 2018. His research interests include multilevel converters topology, predictive control for power converters and electrical drives and their applications in renewable energy systems.

1 Introduction

Power electronics play an important role in renewable energy systems such as wind power generation, fuel cells and solar photovoltaic (PV) system (Rezaei and Mehran, 2019; Li et al., 2019). During the past decade, the Z-source inverter (ZSI) is considered to be an interesting solution compared with the traditional voltage source inverter thanks to its advantages: capability to boot the DC voltage input and overcoming the drawback of short-circuit effect in switching device (Liu et al., 2016; Siwakoti et al., 2015). By improving the ZSI topology, the quasi Z-source inverter (qZSI) is expected to be suitable for PV system applications due to its ability to achieve the continuous input current and decreasing the capacitor voltage stress (Liu et al., 2016, 2014; Anderson and Peng, 2008).

Most of existing control methods use conventional linear controllers and modulation techniques to generate the switching signal of the inverter. In general, the control strategy of the qZSI includes two control schemes for AC and DC sides. The voltage on the DC side is controlled directly by the DC-bus voltage (Ding et al., 2007a) or indirectly by the capacitor voltage (Sen and Elbuluk, 2010; Ding et al., 2007b). With regard to the AC side, the multiple control loops (Li et al., 2013; Gajanayake et al., 2007) with inner current and outer voltage are used to control the output current or voltage. However, it has a low dynamic performance and its performances depend on the quality of the internal current controller. In this method, the state-space averaged or small-signal model is employed to design the proportional-integral (PI) regulators. This implies that it is necessary to tune the gains of the controllers in the whole operating conditions. Another drawback of this technique is a presence of non-minimum phase phenomenon in the DC side, leading to an instability of the whole system. In order to overcome these problems, nonlinear control techniques have been developed for qZSI such as fuzzy (Abu-Rub et al., 2013), sliding mode (Shinde et al., 2017), and neural network (Rostami and Khaburi, 2010). Comparing to the conventional PI controllers, these approaches provide a fast dynamic transient and improved stability. Nonetheless, the disadvantage of these methods is the increase in design complexity.

Nowadays, model predictive control (MPC) has been considered as an alternative and a powerful control methods for power electronics applications (Rodriguez et al., 2013; Kouro et al., 2009; Ngo et al., 2016; Mohamed et al., 2015). In particular, the finite control set model predictive control (FCS-MPC) is among the most widely applied to qZSI thanks to its concept simplicity (without cascaded control loop structure and modulation block) and easy implementation (Mosa et al., 2013; Mo et al., 2011; Karamanakos et al., 2018; Mosa et al., 2017; Bakeer et al., 2015; Ngo et al., 2019). The principal benefit of FCS-MPC is that the non-linearities in the multiple input multiple output systems, constraints and delay compensation can be incorporated directly into the controller. In this case, the cost function for qZSI consists of load current, inductor current, and a capacitor voltage. Then, its minimisation is carried out to obtain the best switching state which is implemented to the inverters. However, the big challenge of the FCS-MPC is the computational burden. In fact, in the FCS-MPC, all switching states of the inverters have to be calculated online for the evaluation of the cost function to achieve the optimal value, leads to increase the calculation time, especially with high number of switching state and long prediction horizons. To address this issue, a parallel algorithm of FCS-MPC for qZSI connected RL load is proposed in Mosa et al. (2014) which decreases the computational time by using the high performance of field programmable gate array (FPGA). Another method is proposed in Bakeer et al. (2016) based on using the sub-cost function of inductor current to select the optimal switching

state for shoot-through (ST) and non-ST cases. As a result, comparing with the conventional FCS-MPC, the amount of calculation of this approach is reduced and the selection of the weighting factors is simplified since the cost function consists of only one weighting factor. However, the high processor and cost are the major disadvantage of their techniques. In Ayad et al. (2017) a branch-and-bound strategy with a move blocking scheme for the optimisation problem is employed to reduce the execution time of the MPC algorithm. Nevertheless, these methods only focused on the reduction of computational cost, not taking into account the stability analysis of the system. With the purpose of address the stability issue, a Lyapunov function based on an FCS model (Kwak et al., 2014; Akter et al., 2016) is proposed for the three-phase two-level voltage source converter. Their solutions are based on the voltage reference vector in the cost function to reduce the computational time. However, the current solution to the qZSI is inefficient due to the presence of ST and non-ST cases in the dynamic system. In Aguilera and Quevedo (2013, 2015) the authors investigated the stability condition in a restricted set with an explicit solution for the optimisation problem. Unfortunately, these strategies are appropriate for the convex MPC. Another technique suggested in Mohamed et al. (2019) and Novak and Dragicevic (2020) used the artificial natural network-based MPC for voltage source inverter to enhance the control performance and reduce the computational burden. Although this approach is interesting, it fails to take into account the stability issue.

Although several studies have been devoted to computational burden, less attention has been paid to consider the stability of the FCS-MPC method. Motivated by the benefits of the classical method in Bakeer et al. (2016), we here propose an efficient model predictive control for qZSI by taking into account the computational delay and incorporating the stability in the control design. A dynamic model of the qZSI is used to predict the performance of the load current, inductor current and capacitor voltage for both ST and non-ST cases. A control horizon of modified one-step prediction is employed to compensate the computational delay, resulting in an improved system performance. The control objective is accomplished through a defined cost function. In this paper, with the aim to guarantee the stability of the closed-loop system, a control Lyapunov function is proposed where only candidate switching states satisfying the stability conditions are considered for the evaluation of the main loop optimisation. Consequently, aside from the reinforcement of the stability, the computational cost of the proposed method is decreased with respect to the conventional algorithm, leading to the feasibility of real-time implementation with an increase of high sampling rate. This means that the control performance can be improved by this solution.

The remainder of the paper is structured as follows: the dynamic model of qSZI is presented in Section 2, then the detail of the proposed control scheme based on Lyapunov function is described in Section 3. In Section 4, simulation results are presented and a comparison study with the classical FCS-MPC method is analysed. Finally, the conclusions are outlined in Section 5.

2 Model of quasi Z-source inverter

Figure 1 presents a simplified diagram of a qZSI. The qZSI consists of fifteen valid switching configurations: six active-state vectors, two null-state vectors and seven ST state vectors (Ayad et al., 2017; Mosa et al., 2017; Bakeer et al., 2017). In order to decrease the computational complexity, the redundant states produce the same output voltage vector which can be considered for qZSI: seven for non-ST state and one for ST state (Bakeer et al., 2016). The summary of the switching status created by this topology is given as Table 1.

The inverter output voltage can be represented as:

$$u_{out} = \frac{2}{3}\left(u_{AN} + a u_{BN} + a^2 u_{CN}\right), \tag{1}$$

with $a = e^{j2\pi/3} = -\frac{1}{2} + j\frac{\sqrt{3}}{2}$.

u_{AN}, u_{BN}, and u_{CN} are the phase voltages of the inverter which can be calculated based on switching state S_x and peak value of DC-link voltage U_{inv} as follows:

$$u_{AN} = S_a U_{inv};\ u_{BN} = S_b U_{inv};\ u_{CN} = S_c U_{inv}, \tag{2}$$

where $S_x = \begin{cases} 1 & \text{if upper switch is ON} \\ 0 & \text{if lower switch is ON} \end{cases}$
$x \in \{a, b, c\}$, $U_{inv} = 2U_{C1} - U_{dc}$.

The dynamic model of the load is formulated as:

$$u_{out} = R i_{out} + L\frac{di_{out}}{dt}, \tag{3}$$

where R, L denote the load resistance and inductance. $u_{out} = [u_{AN}\ u_{BN}\ u_{CN}]^T$ and $i_{out} = [i_a\ i_b\ i_c]^T$ represents the load current.

The dynamic model of the load can be expressed in the stationary reference ($\alpha\beta$) frame by taking the Clarke transformation for (3):

$$\begin{aligned} \frac{di_{out\_\alpha}}{dt} &= \frac{1}{L}\left(u_{out\_\alpha} - R i_{out\_\alpha}\right) \\ \frac{di_{out\_\beta}}{dt} &= \frac{1}{L}\left(u_{out\_\beta} - R i_{out\_\beta}\right), \end{aligned} \tag{4}$$

where the output voltage in the $\alpha\beta$ frame is obtained by the peak DC-bus voltage U_{inv} and the switching status of qZSI S_x:

$$\begin{aligned} u_{out\_\alpha} &= \frac{1}{3} U_{inv}\left(2S_a - S_b - S_c\right) \\ u_{out\_\beta} &= \frac{\sqrt{3}}{3} U_{inv}\left(S_b - S_c\right). \end{aligned} \tag{5}$$

In order to reduce the number of state variables, considering the symmetry of the network ($i_{L1} = i_{L2}$, $u_{C1} = u_{C2}$), the continuous-time model of the capacitor voltage and inductor current depend on the operating condition of the inverter which can be defined as:

a) Non-ST state: (Figure 2(a))

$$\begin{aligned} C_1\frac{du_{C1}}{dt} &= i_{L1} - i_{inv} \\ L_1\frac{di_{L1}}{dt} &= U_{dc} - R_{L1} i_{L1} - u_{C1}, \end{aligned} \tag{6}$$

Figure 1 The configuration of quasi Z-source inverter

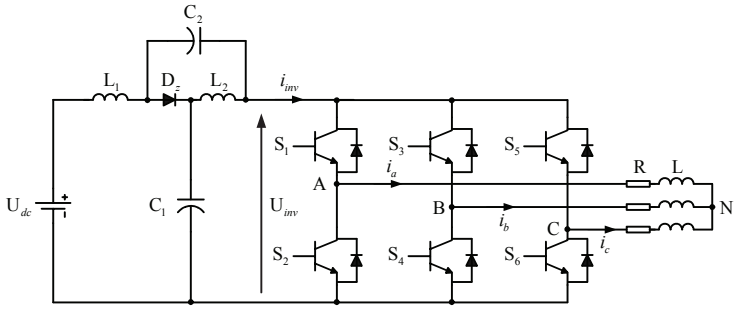

Table 1 Switching status generated by qZSI

Operational state	*Inverter output voltage*	S_1	S_3	S_5	S_2	S_4	S_6
Non-ST states	$U_0 = 0$	0	0	0	1	1	1
	$U_1 = \frac{2}{3}U_{inv}$	1	0	0	0	1	1
	$U_2 = \frac{1}{3}\left(1 + j\sqrt{3}\right)U_{inv}$	1	1	0	0	0	1
	$U_3 = \frac{1}{3}\left(-1 + j\sqrt{3}\right)U_{inv}$	0	1	0	1	0	1
	$U_4 = -\frac{2}{3}U_{inv}$	0	1	1	1	0	0
	$U_5 = \frac{1}{3}\left(-1 - j\sqrt{3}\right)U_{inv}$	0	0	1	1	1	0
	$U_6 = \frac{1}{3}\left(1 - j\sqrt{3}\right)U_{inv}$	1	0	1	0	1	0
ST state	$U_7 = 0$	1	1	1	1	1	1

Figure 2 Simplified representation of the QZSI for non-ST and ST states: (a) non-ST case and (b) ST case

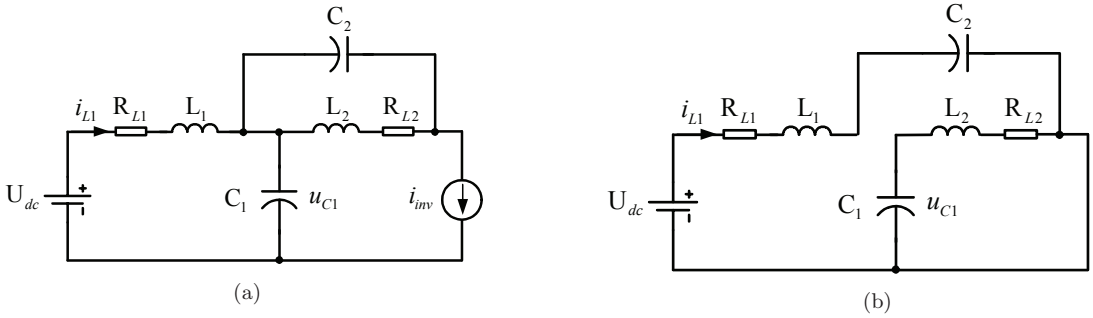

where U_{dc} represents the DC-source voltage and R_{L1}, L_1, C_1 signify the resistance, inductance, and capacitance of the LC network, respectively.

The input current of the inverter i_{inv} is achieved by the load currents and the switching states of inverter:

$$i_{inv} = S_a i_a + S_b i_b + S_c i_c. \tag{7}$$

b) ST state: (Figure 2(b))

$$\begin{aligned} C_1 \frac{du_{C1}}{dt} &= -i_{L1} \\ L_1 \frac{di_{L1}}{dt} &= u_{C1} - R_{L1} i_{L1}. \end{aligned} \tag{8}$$

3 Proposed Lyapunov function-based model predictive control

The main aim of the proposed direct predictive method is to track the load current references $i^*_{out\_\alpha}$ and $i^*_{out\_\beta}$. Moreover, the inductor current i_{L1} and the capacitor voltage u_{C1} are adjusted to their references i^*_{L1} and u^*_{C1} which are derived from the reference calculation. To fulfill these control goals, the cost function of the conventional model predictive control strategy for qZSI is formed by weighting the terms proposed in previous studies (Liu et al., 2016; Mosa et al., 2013; Bakeer et al., 2015):

$$\begin{aligned} g = &\left(i^*_{out\_\alpha} - i^p_{out\_\alpha}\right)^2 + \left(i^*_{out\_\beta} - i^p_{out\_\beta}\right)^2 \\ &+ \lambda_{iL}\left(i^*_{L1} - i^p_{L1}\right)^2 + \lambda_{uC}\left(u^*_{C1} - u^p_{C1}\right)^2, \end{aligned} \tag{9}$$

where λ_{iL}, λ_{uC} denote the weighting factors of inductor current and capacitor voltage.

Based on equations (6) and (8), it is obvious that the prediction value of inductor current has only two values for all possible switching. Therefore, with the aim to reduce the computational burden, a modified FCS-MPC without delay compensation is suggested in Bakeer et al. (2016) which use the sub-cost function outside the main loop optimisation for

the inductor current. In this case, by taking into account the computational delay, the main cost function of control strategy can use the following terms:

$$\begin{aligned} g(u_{k+1}) = &\left(i^*_{out\_\alpha}(k+2) - i^p_{out\_\alpha}(k+2)\right)^2 \\ &+ \left(i^*_{out\_\beta}(k+2) - i^p_{out\_\beta}(k+2)\right)^2 \\ &+ \lambda_{uC}\left(u^*_{C1}(k+2) - u^p_{C1}(k+2)\right)^2. \end{aligned} \tag{10}$$

According to equation (4), considering a sampling time T_s the discrete-time model of the load is achieved by using the forward Euler approximation as follows:

$$\begin{aligned} \hat{i}_{out\_\alpha}(k+1) &= \left(1 - \frac{RT_s}{L}\right) i_{out\_\alpha}(k) \\ &\quad + \frac{T_s}{L} u_{out\_\alpha}(k) \\ i^p_{out\_\alpha}(k+2) &= \left(1 - \frac{RT_s}{L}\right) \hat{i}_{out\_\alpha}(k+1) \\ &\quad + \frac{T_s}{L} u_{out\_\alpha}(k+1) \\ \hat{i}_{out\_\beta}(k+1) &= \left(1 - \frac{RT_s}{L}\right) i_{out\_\beta}(k) \\ &\quad + \frac{T_s}{L} u_{out\_\beta}(k) \\ i^p_{out\_\beta}(k+2) &= \left(1 - \frac{RT_s}{L}\right) \hat{i}_{out\_\beta}(k+1) \\ &\quad + \frac{T_s}{L} u_{out\_\beta}(k+1), \end{aligned} \tag{11}$$

where the components of load current $\hat{i}_{out\_\alpha}(k+1)$ and $\hat{i}_{out\_\beta}(k+1)$ at instant $k+1$ are estimated based on the previous best switching status $u_{out\_\alpha}(k)$, $u_{out\_\beta}(k)$ at instant k. $i^p_{out\_\alpha}(k+2)$, $i^p_{out\_\beta}(k+2)$ are predicted using the estimated values at $k+1$ and all possible switching states of the inverter at time $k+1$.

Approaching equation (6) in the same way, the capacitor voltage and inductor current at the non-ST case can be represented in discrete-time as follows:

$$\begin{aligned} \hat{u}_{C1}(k+1) &= u_{C1}(k) + \frac{T_s}{C_1}\left(i_{L1}(k) - i_{inv}(k)\right) \\ \hat{i}_{L1\_ns}(k+1) &= \left(1 - \frac{R_{L1}T_s}{L_1}\right) i_{L1}(k) \\ &\quad + \frac{T_s}{L_1}\left(U_{dc}(k) - u_{C1}(k)\right) \\ u^p_{C1}(k+2) &= \hat{u}_{C1}(k+1) \\ &\quad + \frac{T_s}{C_1}\left(\hat{i}_{L1\_ns}(k+1) - i^p_{inv}(k+1)\right) \\ i^p_{L1}(k+2) &= \left(1 - \frac{R_{L1}T_s}{L_1}\right) \hat{i}_{L1\_ns}(k+1) \\ &\quad + \frac{T_s}{L_1}\left(U_{dc}(k+1) - \hat{u}_{C1}(k+1)\right), \end{aligned} \tag{12}$$

where the input currents of inverter $i_{inv}(k)$ and $i^p_{inv}(k+1)$ are achieved from equation (7) based on the switching status and the load currents.

Similarly, the discrete-time forms for capacitor voltage and inductor current at ST case can be obtained from equation (8) for one-step prediction as:

$$\begin{aligned} \hat{u}_{C1}(k+1) &= u_{C1}(k) - \frac{T_s}{C_1} i_{L1}(k) \\ \hat{i}_{L1\_s}(k+1) &= \left(1 - \frac{R_{L1}T_s}{L_1}\right) i_{L1}(k) + \frac{T_s}{L_1} u_{C1}(k). \end{aligned} \tag{13}$$

The state errors of the load current and capacitor voltage are assigned as:

$$\widetilde{i}_{out\_\alpha} = i_{out\_\alpha} - i^*_{out\_\alpha},\ \widetilde{i}_{out\_\beta} = i_{out\_\beta} - i^*_{out\_\beta} \tag{14}$$

Replacing equation (14) in equations (4) and (6), thereby obtaining

$$\begin{aligned} \frac{d\widetilde{i}_{out\_\alpha}}{dt} &= \frac{1}{L}\left(u_{out\_\alpha} - Ri_{out\_\alpha}\right) - \frac{di^*_{out\_\alpha}}{dt}, \\ \frac{d\widetilde{i}_{out\_\beta}}{dt} &= \frac{1}{L}\left(u_{out\_\beta} - Ri_{out\_\beta}\right) - \frac{di^*_{out\_\beta}}{dt}, \\ \frac{d\widetilde{u}_{C1}}{dt} &= \frac{1}{C1}\left(i_{L1} - i_{inv}\right) - \frac{du^*_{C1}}{dt}. \end{aligned} \tag{15}$$

Since the sampling frequency ($f_s = 20$ kHz) is too large than the frequency of the load current ($f = 50$ Hz), it is negligible the variation of the load current during the sampling interval. Then, we can assume that:

$$\frac{di^*_{out\_\alpha}}{dt} = 0,\ \frac{di^*_{out\_\beta}}{dt} = 0,\ \frac{du^*_{C1}}{dt} = 0. \tag{16}$$

In this paper, the control Lyapunov candidate function (CLF) is proposed:

$$\begin{aligned} V\left(\widetilde{i}_{out\_\alpha}, \widetilde{i}_{out\_\beta}\right) &= \frac{1}{2}K_\alpha \widetilde{i}^2_{out\_\alpha} + \frac{1}{2}K_\beta \widetilde{i}^2_{out\_\beta} \\ &\quad + \frac{1}{2}K_{uC}\widetilde{u}^2_{C1} \end{aligned} \tag{17}$$

with derivative

$$\begin{aligned} \dot{V}\left(\widetilde{i}_{out\_\alpha}, \widetilde{i}_{out\_\beta}, \widetilde{u}_{C1}\right) &= K_\alpha \widetilde{i}_{out\_\alpha} \frac{d\widetilde{i}_{out\_\alpha}}{dt} \\ &\quad + K_\beta \widetilde{i}_{out\_\beta} \frac{d\widetilde{i}_{out\_\beta}}{dt} + K_{uC}\widetilde{u}_{C1}\frac{d\widetilde{u}_{C1}}{dt}, \end{aligned} \tag{18}$$

where K_α, K_β and K_{uC} denote the positive gains.

The variation of the load current reference is insignificant due to the small sampling time ($T_s = 50$ μs) of the controller. To decrease the computational time, the extrapolation of its value can be simplified as:

$$i^*_{out\_\alpha}(k+2) = i^*_{out\_\alpha}(k),\ i^*_{out\_\beta}(k+2) = i^*_{out\_\beta}(k). \tag{19}$$

In a practical system, delay compensation is required for implementation due to the computational time and the communication time (Geyer and Quevedo, 2015; Rodriguez and Cortes, 2012; Vazquez et al., 2017). With the aim to reduce the prediction error due to computational delay and improve the performance of the system, one common compensation technique (Rodriguez and Cortes, 2012; Vazquez et al., 2017; Kouro et al., 2009) is based on estimating the value at instant $k+1$ utilising the previous switching status at time k. Then, the optimal switching status that is obtained from

Figure 3 Computational cost reduction in the loop optimisation of the proposed method: (a) the improved MPC algorithm with reduced candidate sequences and delay compensation and (b) the prediction derivative of Lyapunov function for all switching status (see online version for colours)

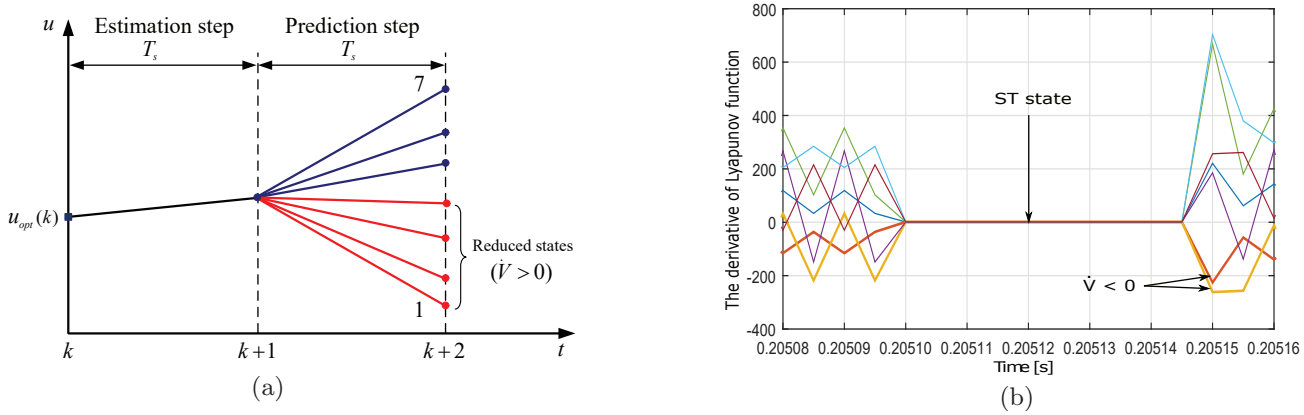

minimising the cost function at time $k+2$ is applied to qZSI. Consequently, a large amount of computational calculation makes it difficult to execute the algorithm with a high sampling rate in real-time. In order to address this issue, the modified algorithm is proposed in Bakeer et al. (2016) for reducing the computational cost and simplifying the selection of weighting factor. Approaching this method and achieving a significant reduction of computational burden, a pruning approach is imposed to select the available finite set of controls based on the decrease of the Lyapunov function V (17). Under this circumstance, two cases are considered for the cost function optimisation: the first one corresponds to the ST state and the second one is the non-ST state. In the first one, the ST state is selected as the optimal switching state by comparing the sub-cost function as illustrated in Figure 3(b) (for example at time $t = 0.20512$ s). In this case, the criteria function of the inductor current is recognised as a key to solve the optimisation problem (see Algorithm 1). On the contrary, at each prediction interval, the derivative of the Lyapunov function $\dot{V}$ is evaluated with all possible switching states of the inverter. As illustrated in Figure 3(b), ones a predictive switching status is determined to pass a stability criterion ($\dot{V} < 0$), then this viable alternative is chosen for the evaluation of the main cost function. As highlighted in Figure 3(b), there are some unstable switching states which can be eliminated for the prediction and loop optimisation. For instance, at the time $t = 0.20515$ s, there are only two switching states which are selected for optimisation. Although the increase of evaluation for the Lyapunov function is unexpected, the computational burden of the proposed approach is decreased with respect to the classical method. Table 2 summarises the comparison of the necessary amount of calculation between the previous FCS-MPC and the proposed method. It is clear to note that the proposed algorithm is improved by reducing the candidate control input for prediction and enumeration of the cost function instead of evaluating all considered switching states. Consequently, our technique provides additional support for long prediction horizon and multilevel inverter. Furthermore, this method represents a valuable alternative to link the stability guarantees of the closed-loop system with the optimisation problem. The best sequence of control input $u_{opt} = [S_a \ S_b \ S_c]^T$ is obtained from minimising the cost function below:

$$u_{opt} = \arg\left\{\min_{u_{k+1}\in\{0,1\}^3} g\left(u_{k+1}\right)\right\} \quad \text{subject to } \dot{\mathrm{V}}(\mathrm{k}+1) < 0 \tag{20}$$

It is worthwhile to mention that the selection is not redundant with the optimisation MPC problem. In this case, control performance can be decreased due to the consideration of the stability in the optimisation problem. This is the price to be paid to ensure a Lyapunov decrease by minimising the cost function. Therefore, the stability of the closed-loop system is always guaranteed for all operating circumstances. Finally, the proposed control technique is described as Algorithm 1.

Algorithm 1 Algorithm of model predictive control based on Lyapunov function for qZSI

Input: $i_a(k)$, $i_b(k)$, $i_c(k)$, $U_{dc}(k)$, $u_{C1}(k)$, $i_{L1}(k)$, $i^*_{out\_\alpha}(k)$, $i^*_{out\_\beta}(k)$, $i^*_{L1}(k)$ and $u^*_{C1}(k)$
Output: S_a, S_b, S_c
Estimate $U_{inv}(k)$, $i_{inv}(k)$ from (2) and (7)
Initialize x_{opt}, g_{opt}
Calculate $\hat{i}_{out\_\alpha}(k+1)$, $\hat{i}_{out\_\beta}(k+1)$ using (1), (2) and (11)
Predict $\hat{i}_{L1\_ns}(k+1)$, $\hat{i}_{L1\_s}(k+1)$, $\hat{u}_{C1}(k+1)$ using (12), (13)
if $\left(i^*_{L1}(k+1) - \hat{i}_{L1\_s}(k+1)\right)^2 < \left(i^*_{L1}(k+1) - \hat{i}_{L1\_ns}(k+1)\right)^2$ **then**
    $x_{opt} = 8$
else
    for $i = 1$ to 7 **do**
        Calculate $u_{out\_\alpha}(k+1)$, $u_{out\_\beta}(k+1)$ from (1) and (2)
        Evaluate $\dot{V}(k+1)$ based on (15) and (18)
        if $\dot{V}(k+1) < 0$ **then**
            Predict $i^p_{out\_\alpha}(k+2)$, $i^p_{out\_\beta}(k+2)$ from (12)
            Predict $u^p_{C1}(k+2)$ based on (12)
            Compute $g(u_{k+1})$ from (10)
            if $g(u_{k+1}) < g_{opt}$ **then**
                $g_{opt} = g(u_{k+1}); x_{opt} = i$
Store x_{opt}

Figure 4 Transient response and FFT of the load current for the classical FCS-MPC and proposed method: (a) three-phase load current of the conventional algorithm; (b) three-phase load current of the proposed method; (c) FFT of the load current for the conventional algorithm and (d) FFT of the load current for the proposed method (see online version for colours)

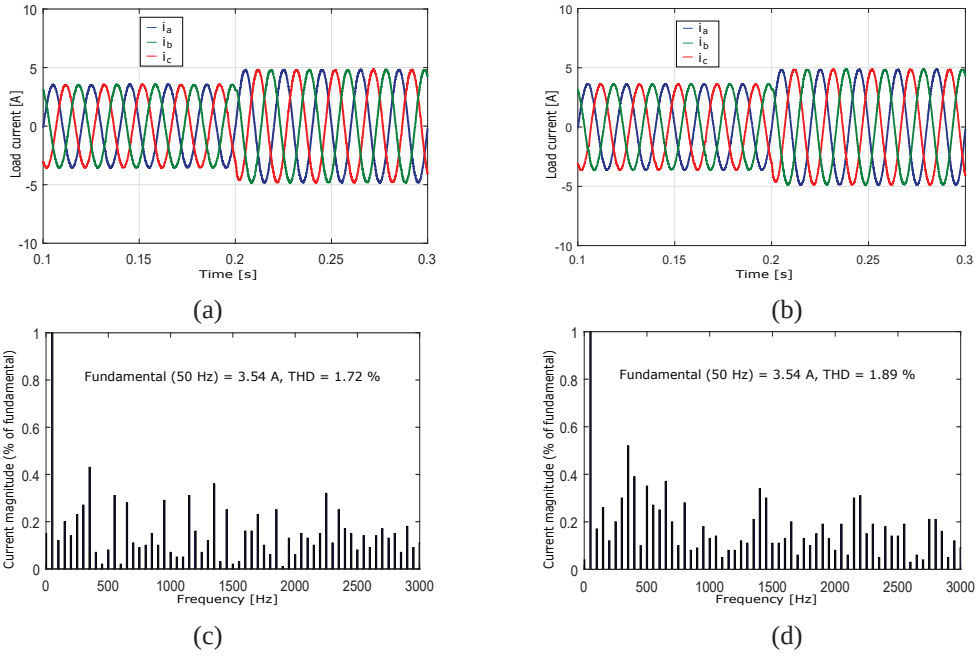

4 Simulation results

In order to prove the validation of the proposed control strategy, the simulation using Matlab/Simulink software are carried out under different conditions of the reference. Table 3 summarises the simulation parameters of the system.

Table 2 Comparison of computational cost of two controllers

Variables	*Classical FCS-MPC*	*Proposed method*
$\hat{i}_{out\_\alpha}(k+1), \hat{i}_{out\_\beta}(k+1)$	1	1
$\hat{i}_{L1\_ns}(k+1)$	1	1
$\hat{i}_{L1\_s}(k+1)$	1	1
$\hat{u}_{C1}(k+1)$	1	1
$u_{out\_\alpha}(k+1), u_{out\_\beta}(k+1)$	7	7
$i^p_{out\_\alpha}(k+2), i^p_{out\_\beta}(k+2)$	7	3
$u^p_{C1}(k+2)$	7	3
$g(u_{k+1})$	7	3
$\dot{V}(k+1)$	0	7
Total	*32*	*27*

To estimate the average frequency inverter obtained by the FCS-MPC, the following formulation recommended in Rodriguez and Cortes (2012) can be employed:

$$f_{sw} = \frac{f_{sw\_A} + f_{sw\_B} + f_{sw\_C}}{3} = \frac{n_{sw\_A} + n_{sw\_B} + n_{sw\_C}}{3T_{sim}}, \quad (21)$$

where n_{sw_A}, n_{sw_B}, and n_{sw_C} indicate the number of commutation in the control signals of three inverter's branches by measuring over a simulation time (T_{sim}).

Table 3 Parameters for simulation investigation

Parameter	*Value*	*Description*
U_{dc}	70 [V]	DC-source voltage
f	50 [Hz]	Frequency of load current
R_{L1}	0.1 [Ω]	Resistance of inductor
L_1	2 [mH]	Inductance of inductor
C_1	480 [μF]	DC capacitance
R	12 [Ω]	Load resistance
L	24 [mH]	Load inductance
T_s	50 [μs]	Sampling time of control method
λ_{uC}	1.2	Weighting factor of capacitor voltage
K_α, K_β, K_{uC}	1.5	Positive gains

The reference of load current is obtained from the desired output power as $i^*_{out} = \sqrt{2P^*_{out}/3R}$. Ignoring the power losses in the inverter and filter, the inductor current reference is calculated based on the output power $i^*_{L1} = P^*_{out}/U_{dc}$. For the simplicity, the capacitor voltage reference should more than double than the peak phase output voltage according to Li et al. (2013).

The results achieved from the conventional algorithm of MPC (Bakeer et al., 2016) is introduced in this research to study better the effectiveness of the proposed method. To generate the same $f_{sw} = 6$ kHz, the sampling time of the MPC is considered $T_s = 50$ μs. The designed output power (P^*_{out}) is stepped from 250 W to 450 W at instant $t = 0.25$ s, while the reference of peak phase load current and inductor current are changed from 3.7 A to 4.95 A and from 3.6 A to 6.42 A, respectively. The capacitor voltage reference is kept at 120 V. Figure 4(b) shows the dynamic response of three-phase load current for the proposed technique. In particular, comparing with the classical FCS-MPC method,

Figure 5 Performance of load current, inductor current, capacitor voltage and DC-link voltage: (a) phase current; (b) inductor current; (c) capacitor voltage and (d) zoom of DC-link voltage (see online version for colours)

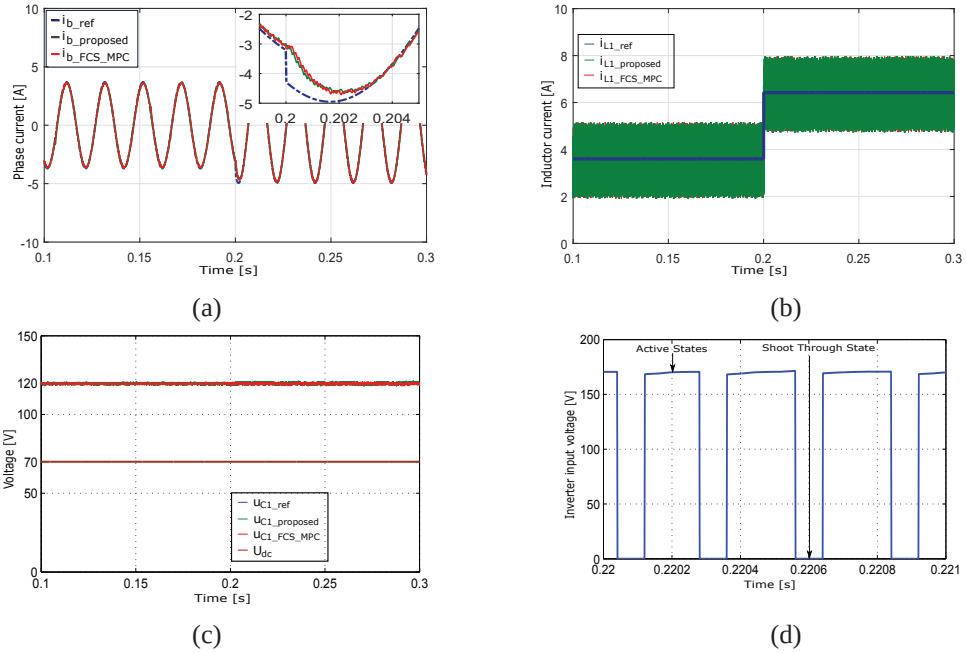

the proposed method achieves the same performance of the load current as illustrated in Figure 4(a) and (b). It can be seen from Figure 5 that the proposed method obtains an accurate current tracking ability and reach its steady state within a short transient response time. Further, by using Powergui Fast Fourier Transform (FFT) toolbox, the harmonic spectra of the load current for the conventional algorithm and proposed method are also analysed and compared in Figures 4(c) and (d). As shown in these figures, the total harmonic distortion (THD) of the current for the proposed method increases slightly from 1.72% to 1.89% compared with the classical FCS-MPC algorithm. On the other hand, the proposed method is capable to track the capacitor voltage as illustrated in Figure 5(c), leading to the peak DC-link voltage of 170 V (Figure 5(d)). Figure 5(d) presents the shaped pulse voltage to illustrate the capability of boot DC voltage input. In addition, the inductor current is maintained at its reference value as shown in Figure 5(b).

Figure 6 Number of switching states for main optimisation loop (see online version for colours)

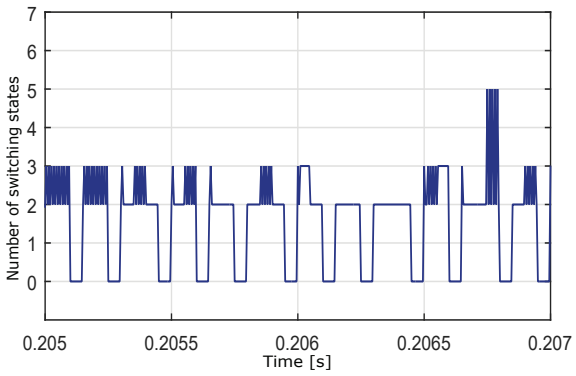

Table 4 Comparison of two controllers for one-step horizon with delay compensation

	Method	
Performance	*Conventional algorithm*	*Proposed method*
THD of i_a with $P_0 = 250$ W	1.72%	1.89%
THD of i_a with $P_0 = 450$ W	1.66%	1.67%
Average prediction states considered for loop optimisation	7	3
Average computation time	28 µs	23 µs

As previously mentioned, seven predictions of switching state at non-ST case have to be evaluated in the main cost function for the algorithm proposed in Bakeer et al. (2016). On the contrary, the average predictions considered of loop optimisation are only 3 for the proposed method (see Figure 6). The computational cost depends on the measured states and the references. The simulation result indicates that the maximum and minimum switching states for evaluating the main cost function are 5 and 2, respectively. As a result, the proposed method is more attractive from the perspective of the computational cost compared with the classical FCS-MPC method. To show the computational efficiency of the proposed strategy, we test the algorithm by employing the S-function block in the Simulink with embedded coder tools. The function tic-toc of Matlab is utilised to estimate the computation time. In fact, the average computation time of the classical method is about 28 µs while the proposed method requires only 23 µs in a 2.2 GHz, i5-5200 CPU. The detail comparisons of two controllers, comprehending the THD of the load current and computation time are reported in Table 4. The most striking observation to emerge from the data comparison was

Figure 7 Simulation results with parameter variation: (a) waveform of three-phase load current; (b) steady-state of capacitor voltage and (c) steady-state of inductor current (see online version for colours)

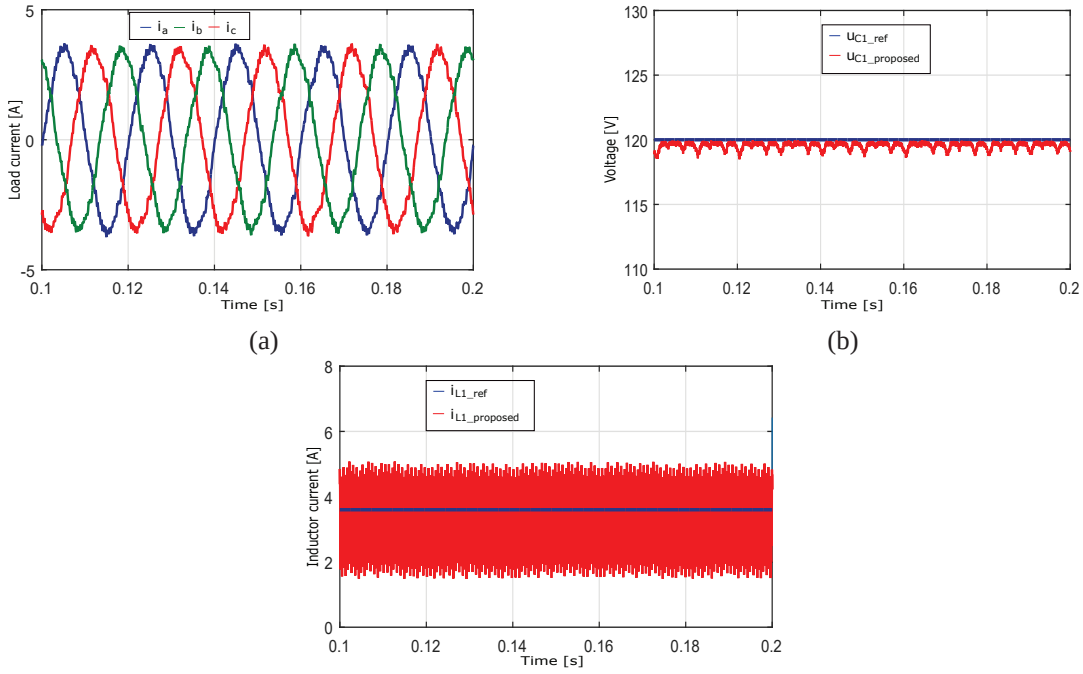

(a) (b) (c)

Figure 8 Performance of proposed method under step change in DC input voltage: (a) dynamic response of DC input and capacitor voltages and (b) three-phase load current waveform (see online version for colours)

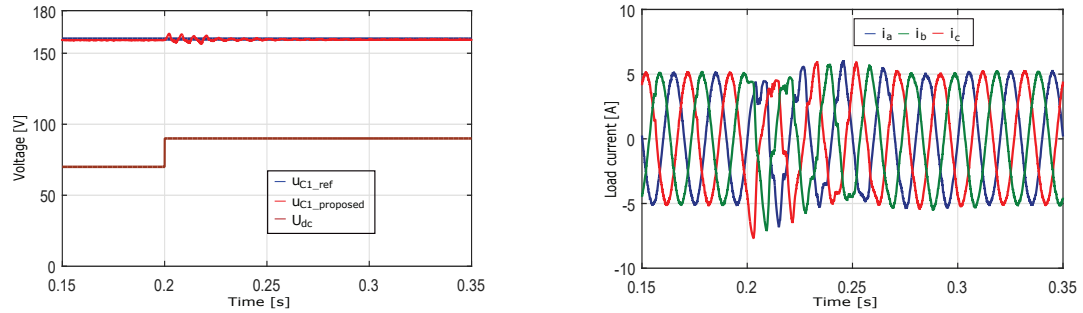

(a) (b)

the assurance of the closed-loop stability and decrease in computational load. Consequently, our study provides the framework for a new way to support the feasibility of the real-time FCS-MPC implementation with a lower processor and long prediction horizon.

To confirm the robustness of the controller against parameter variations, an examination with an increase of 50% in the load resistance and inductance is conducted in our study. Figure 7 illustrates the results of the proposed method under parameter variations. It can be observed that the proposed method is continued to reach the desired values of inductor current and capacitor voltage with small deviations. The THD of the load current increases from 3.11% to 4.6% but it still meets within the limit required of the IEEE 519 standard.

Nowadays, the qZSI is recognised as a suitable topology for PV system. In this case, the DC input voltage is incorporated into PV system, leading to the variation of the DC voltage due to the change of the weather. In order to investigate the performance of the proposed scheme under this circumstance, the DC input voltage is changed from 70 V to 90 V at instant $t = 0.2$ s, while the load current and capacitor voltage are kept at 5.3 A ($P_0 = 500$ W) and 160 V, respectively. As can be seen in Figure 8, the capacitor voltage and load current return their references after the transient time in spite of the step change in DC input voltage.

5 Conclusion

This paper introduces a computationally efficient model predictive control approach for qZSI. With the aim to solve the challenges of using FCS-MPC for qZSI, the development of FCS-MPC based on the Lyapunov function is proposed in this technique. At each sampling time, only available switch state that guarantees the stability criteria is taken into account in the optimisation problem. As a result, the computation

time of the proposed method is reduced by 18% compared with the classical FCS-MPC algorithm thanks to stability consideration, facilitating the implementation of the MPC method in real-time applications. In order to illustrate the effectiveness of the control strategy, a comparative study between the proposed method and conventional FCS-MPC is investigated. The simulation results validate the feasibility of the proposed method in regard to THD of load current and computational burden. To further our research, we intend to implement the proposed strategy in a real-time system.

References

Abu-Rub, H., Iqbal, A., Ahmed, S.M., Peng, F.Z., Li, Y. and Baoming, G. (2013) 'Quasi-Z-source inverter-based photovoltaic generation system with maximum power tracking control using Anfis', *IEEE Transactions on Sustainable Energy*, Vol. 4, No. 1, pp.11–20.

Aguilera, R.P. and Quevedo, D.E. (2013) 'Stability analysis of quadratic MPC with a discrete input alphabet', *IEEE Transactions on Automatic Control*, Vol. 58, No. 12, pp.3190–3196.

Aguilera, R.P. and Quevedo, D.E. (2015) 'Predictive control of power converters: designs with guaranteed performance', *IEEE Transactions on Industrial Informatics*, Vol. 11, No. 1, pp.53–63.

Akter, M., Mekhilef, S., Tan, N. and Akagi, H. (2016) 'Modified model predictive control of a bidirectional AC–DC converter based on Lyapunov function for energy storage systems', *IEEE Transactions on Industrial Electronics*, Vol. 63, No. 2, pp.704–715.

Anderson, J. and Peng, F. (2008), Four quasi-Z-Source inverters', *IEEE Power Electronics Specialists Conference*, Rhodes, Greece, pp.2743–2749.

Ayad, A., Karamanakos, P. and Kennel, R. (2017) 'Direct model predictive current control strategy of quasi-Z-source inverters', *IEEE Transactions on Power Electronics*, Vol. 32, No. 7, pp.5786–5801.

Bakeer, A., Ismeil, M. and Orabi, M. (2016) 'A powerful finite control set-model predictive control algorithm for quasi Z-source inverter', *IEEE Transactions on Industrial Informatics*, Vol. 12, No. 4, pp.1371–1379.

Bakeer, A., Ismeil, M. and Orabi, M. (2017) 'Modified finite control set-model predictive controller (MFCS-MPC) for quasi Z-source inverters based on a current observer', *Journal of Power Electronics*, Vol. 17, No. 3, pp.610–620.

Bakeer, A., Ismeil, M., Kouzou, A. and Orabi, M. (2015) 'Development of MPC algorithm for quasi Z-source inverter (qZSI)', *3rd International Conference on Control, Engineering Information Technology (CEIT)*, Tlemcen, Algeria, pp.1–6.

Ding, X., Qian, Z., Yang, S., Cui, B. and Peng, F. (2007a) 'A direct peak DC-link boost voltage control strategy in Z-source inverter', *Twenty-Second Annual IEEE Applied Power Electronics Conference and Exposition*, Anaheim, CA, USA, pp.648–653.

Ding, X., Qian, Z., Yang, S., Cui, B. and Peng, F. (2007b) 'A PID control strategy for DC-link boost voltage in Z-source inverter', *Twenty-Second Annual IEEE Applied Power Electronics Conference and Exposition*, Anaheim, CA, USA, pp.1145–1148.

Gajanayake, C., Vilathgamuwa, D. and Loh, P. (2007) 'Development of a comprehensive model and a multiloop controller for Z-source inverter DG systems', *IEEE Transactions on Industrial Electronics*, Vol. 54, No. 4, pp.2352–2359.

Geyer, T. and Quevedo, D. (2015) 'Performance of multistep finite control set model predictive control for power electronics', *IEEE Transactions on Power Electronics*, Vol. 30, No. 3, pp.1633–1644.

Karamanakos, P., Ayad, A. and Kennel, R. (2018) 'A variable switching point predictive current control strategy for quasi-z-source inverters', *IEEE Transactions on Industry Applications*, Vol. 54, No. 2, pp.1469–1480.

Kouro, S., Cortes, P., Vargas, R., Ammann, U. and Rodriguez, J. (2009) 'Model predictive control-A simple and powerful method to control power converters', *IEEE Transaction On Industrial Electronics*, Vol. 56, No. 6, pp.1826–1838.

Kwak, S., Yoo, S. and Park, J. (2014) 'Finite control set predictive control based on Lyapunov function for three-phase voltage source inverters', *IET Power Electronics*, Vol. 7, No. 11, pp.2726–2732.

Li, H., Bai, J., Kanae, S., Li, Y. and Yue, L. (2019) 'Active disturbance rejection control of three-phase grid-connected photovoltaic systems', *International Journal of Modelling, Identification and Control*, Vol. 33, No. 3, pp.225–236.

Li, Y., Jiang, S., Cintron-Rivera, J. and Peng, F. (2013) 'Modeling and control of quasi-Z-source inverter for distributed generation applications', *IEEE Transactions on Industrial Electronics*, Vol. 60, No. 4, pp.1532–1541.

Liu, Y., Abu-Rub, H. and Ge, B. (2014) 'Z-source/Quasi-Z-source inverters: derived networks, modulations, controls, and emerging applications to photovoltaic conversion', *IEEE Industrial Electronics Magazine*, Vol. 8, No. 4, pp.32–44.

Liu, Y., Abu-Rub, H., Ge, B., Blaabjerg, F., Ellabba, O. and Loh, P.C. (2016) *Impedance Source Power Electronic Converters*, Wiley-IEEE Press, John Wiley & Sons, UK.

Mo, W., Loh, P.C. and Blaabjerg, F. (2011), Model predictive control for Z-source power converter', *8th International Conference on Power Electronics - ECCE Asia*, Jeju, South Korea, pp.3022–3028.

Mohamed, I., Rovetta, S., Do, T., Dragicević, T. and Diab, A. (2019) 'A neural-network-based model predictive control of three-phase inverter with an output LC filter', *IEEE Access*, Vol. 7, pp.124737–124749.

Mohamed, I., Zaid, S., Abu-Elyazeed, M. and Elsayed, H. (2015) 'Improved model predictive control for three-phase inverter with output LC filter', *International Journal of Modelling, Identification and Control*, Vol. 23, No. 4, pp.371–379.

Mosa, M., Balog, R. and Abu-Rub, H. (2017) 'High-performance predictive control of quasi-impedance source inverter', *IEEE Transactions on Power Electronics*, Vol. 32, No. 4, pp.3251–3262.

Mosa, M., Dousoky, G. and Rub, H. (2014), A novel FPGA implementation of a model predictive controller for SiC-based Quasi-Z-source inverters', *IEEE Applied Power Electronics Conference and Exposition – APEC 2014*, Fort Worth, TX, USA, pp.1293–1298.

Mosa, M., Ellabban, O., Kouzou, A., Abu-Rub, H. and Rodriguez, J. (2013) 'Model predictive control applied for quasi-z-source inverter', *Twenty-Eighth Annual IEEE Applied Power Electronics Conference and Exposition (APEC)*, Long Beach, CA, USA, pp.165–169.

Ngo, B., Ayerbe, P., Olaru, S. and Niculescu, S. (2016) 'Model predictive power control based on virtual flux for grid connected three-level neutral-point clamped inverter', *18th European Conference on Power Electronics and Applications (EPE'16 ECCE Europe)*, Karlsruhe, Germany, pp.1–10.

Ngo, V., Nguyen, M., Tran, T., Lim, Y. and Choi, J. (2019) 'A simplified model predictive control for T-type inverter with output LC filter', *Energies*, Vol. 12, p.31, https://doi.org/10.3390/en12010031

Novak, M. and Dragicevic, T. (2020) 'Supervised imitation learning of finite set model predictive control systems for power electronics', *IEEE Transactions on Industrial Electronics*, pp.1–1.

Rezaei, N. and Mehran, K. (2019) 'A model-based implementation of an MPPT technique and a control system for a variable speed wind turbine PMSG', *International Journal of Modelling, Identification and Control*, Vol. 31, No. 1, pp.3–15.

Rodriguez, J. and Cortes, P. (2012), *Predictive Control of Power Converters and Electrical Drives*, John Wiley & Sons, UK.

Rodriguez, J., Kazmierkowski, M.P., Espinoza, J.R., Zanchetta, P., Abu-Rub, H., Young, H.A. and Rojas, C.A. (2013) 'State of the art of finite control set model predictive control in power electronics', *IEEE Transactions on Industrial Informatics*, Vol. 9, No. 2, pp.1003–1016.

Rostami, H. and Khaburi, D. (2010), Neural networks controlling for both the DC boost and AC output voltage of Z-source inverter', *1st Power Electronic Drive Systems Technologies Conference (PEDSTC)*, Tehran, Iran, pp.135–140.

Sen, G. and Elbuluk, M.E. (2010) 'Voltage and current-programmed modes in control of the Z-source converter', *IEEE Transactions on Industry Applications*, Vol. 46, No. 2, pp.680–686.

Shinde, U., Kadwane, S., Gawande, S., Reddy, M. and Mohanta, D. (2017) 'Sliding mode control of single-phase grid-connected quasi-Z-source inverter', *IEEE Access*, Vol. 5, 10232–10240.

Siwakoti, Y.P., Peng, F.Z., Blaabjerg, F., Loh, P.C., Town, G.E. and Yang, S. (2015) 'Impedance-source networks for electric power conversion Part II: review of control and modulation techniques', *IEEE Transactions on Power Electronics*, Vol. 30, No. 4, pp.1887–1906.

Vazquez, S., Rodriguez, J., Rivera, M., Franquelo, L. and Norambuena, M. (2017) 'Model predictive control for power converters and drives: advances and trends', *IEEE Transactions on Industrial Electronics*, Vol. 64, No. 2, pp.935–947.